



## Gadolinium and Thulium Doping to Perovskite Structured Strontium Titanates at Strontium and Titanium Sites

RAMANJEET KAUR<sup>1\*</sup> and ANAND K TYAGI<sup>2</sup>

<sup>1</sup>Department of Applied Sciences, SBSSTC, I. K. Gujral Punjab Technical University, Kapurthala, 144603 (Punjab) India.

<sup>2</sup>Vice Chancellor, Mahatma Gandhi Kashi Vidyapith, Varanasi (UP) India.

\*Corresponding author E-mail: ramanjeetgill99@gmail.com, anandktyagi@gmail.com

<http://dx.doi.org/10.13005/ojc/380112>

(Received: June 07, 2021; Accepted: January 01, 2022)

### ABSTRACT

Low temperature sol gel novel technique has been employed, in the work here, to fabricate gadolinium and thulium doped strontium titanates with nominal composition;  $\text{Sr}_{1-a}\text{Gd}_a\text{Ti}_{1-b}\text{Tm}_b\text{O}_{3-6}$  for various values of 'a' and 'b'. The synthesized ceramics were cubic structured, phase pure, having well developed morphology and desired composition as revealed by XRD and FESEM/EDX characterization techniques. The electrical and dielectric properties of the prepared samples were studied and various parameters like dielectric constant, loss factor, a c conductivity etc. were determined. Furthermore, these properties enhance with gadolinium and thulium doping at strontium and titanium sites respectively.

**Keywords:** Thulium, Strontium titanates, Perovskite, Gadolinium.

### INTRODUCTION

Nowadays, fuel cells are emerging as a leading technology in the field of power generation owing to their better efficiency and environment friendliness. A fuel cell produces electric current via electrochemical reaction using hydrogen, oxygen as fuels and producing water as by product. Out of various types of fuel cell used nowadays, solid oxide fuel cells (SOFCs) are preferred due to various limitations suffered by counter fuel cells like requirement of pure fuel, expensive catalyst, corrosive electrolyte, high temperature requirement etc<sup>1-2</sup>.

Among various conventional materials employed in fabrication of SOFCs i.e. Ni-Cu/YSZ (nickel/copper-yttria stabilized zirconia), rare earth doped  $\text{CeO}_2$  (ceria), perovskite structured oxides etc. Lanthanum chromites, Strontium titanates etc.; both in pure and derived forms, are leading candidates in perovskite structured oxides<sup>3-4</sup>. The investigation of electrical properties of strontium titanates doped at 'Sr' and 'Ti' sites reveals the enhancement in the ionic conductivity with doping<sup>5-6</sup>. The doped strontium titanates have been widely employed in fabrication of various components of SOFCs i.e. anode, cathode and electrolytes. These oxides offers many advantages over other materials like high stability in oxygen,



carbon, and sulfur containing atmospheres, remarkably active for methane ( $\text{CH}_4$ ) oxidation at high temperature in the absence of excess steam, high conductivity (mainly in doped forms) stable dimensionally and chemically upon redox cycling etc<sup>7-9</sup>.

In this study, gadolinium and thulium have been doped at strontium and titanium sites respectively for various compositions via sol gel route; furthermore, structural, morphological and electrical/dielectric properties of the fabricated samples were studied.

## EXPERIMENTAL

$\text{Sr}_{1-a}\text{Gd}_a\text{Ti}_{1-b}\text{Tm}_b\text{O}_{3-\delta}$  ( $a = 0, b = 0$ ;  $a = 0.05, b = 0.005$  and  $a = 0.1, b = 0.005$ ) samples had been synthesized via sol gel method with the help of  $\text{Ti}(\text{OC}_3\text{H}_7)_4$ ,  $\{\text{Sr}(\text{CH}_3\text{COO})_2\}$ ,  $\{\text{Gd}(\text{NO}_3)_3 \cdot 6\text{H}_2\text{O}\}$  and  $\{\text{Tm}(\text{NO}_3)_3 \cdot 5\text{H}_2\text{O}\}$  as metal precursors; propanol, hydrochloric acid (HCl) and distilled water as solvents. Here, in this series, three samples were synthesized for various combinations of 'a' and 'b' i.e.  $a = 0, b = 0$ ;  $a = 0.05, b = 0.005$  and  $a = 0.1, b = 0.005$ , and were named as SGTT0, SGTT1 and SGTT2 respectively employing the sol gel technique<sup>10</sup>. The calcination and then sintering of derived powder samples were carried out at  $600^\circ\text{C}$  and  $1250^\circ\text{C}$  respectively for 2 h; afterwards the powders were pelletized and pellets were further heated at  $600^\circ\text{C}$  for 1 hour.

X-ray diffraction, SEM and dielectric characterization of the prepared samples were carried out using XPERT-PRO X-ray diffractometer, Nova Nano FE-SEM (FEI) and LCR HiTester respectively.

## RESULTS AND DISCUSSION

### XRD Analysis

The Fig. 1 includes the XRD patterns of SGTT samples for all the compositions; the peaks are well defined, properly indexed based on cubic structure symmetry mathematical method<sup>11</sup> and phase pure. Similar XRD patterns have been observed for  $\text{SrTiO}_3$  as reported in literature<sup>10</sup>. All the three XRD patterns are almost identical with slight shift to the large angle with increase in Gadolinium content; the replacement of strontium ions (ionic

radius 132 pm) with smaller gadolinium ions (ionic radius 107.8 pm) may be responsible for that<sup>8,12</sup>.

**Table 1: Lattice Parameter Values for  $\text{Sr}_{1-a}\text{Gd}_a\text{Ti}_{1-b}\text{Tm}_b\text{O}_{3-\delta}$  Samples ( $0 \leq a \leq 0.1, 0 \leq b \leq 0.005$ )**

Sample code	a	b	Lattice Parameter (Å)
SGTT0	0	0	3.9114
SGTT1	0.05	0.005	3.9022
SGTT2	0.1	0.005	3.8984

The lattice parameter values for all the three samples, calculated using mathematical method for cubic crystals<sup>11</sup>, are included in Table 1. The 'a' values decrease with increase in gadolinium content due to replacement of larger strontium ions by smaller gadolinium ions. The crystallite size of prepared samples, calculated for peak (110) using Sherrer's equation<sup>13</sup>, was between 46 to 52nm.

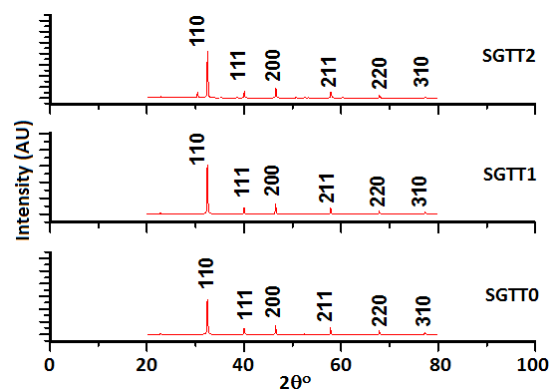


**Fig. 1. XRD Peak Pattern for  $\text{Sr}_{1-a}\text{Gd}_a\text{Ti}_{1-b}\text{Tm}_b\text{O}_{3-\delta}$  Samples ( $0 \leq a \leq 0.1, 0 \leq b \leq 0.005$ ) FESEM Analysis**

FESEM microstructures for doped  $\text{Sr}_{1-a}\text{Gd}_a\text{Ti}_{1-b}\text{Tm}_b\text{O}_{3-\delta}$  samples ( $0 \leq a \leq 0.1, 0 \leq b \leq 0.005$ ) included in Fig. 2, clearly reveal the dense, homogeneous and well crystalline microstructure of the synthesized samples having properly developed grains. The grains are almost spherical, with well defined boundaries, small inter-granular porosity and without any agglomeration. All the prepared samples have almost identical morphology; the only difference lies in the grain size. The grain size range for SGTT0, SGTT1 and SGTT2 was 407-972nm, 83-587nm and 104-750 nm respectively.

EDX analysis revealed that both atomic and weight ratios of constituent elements i.e. Sr, Ti, Tm, Gd and O were close to theoretical values thus confirming the formation of desired compounds.

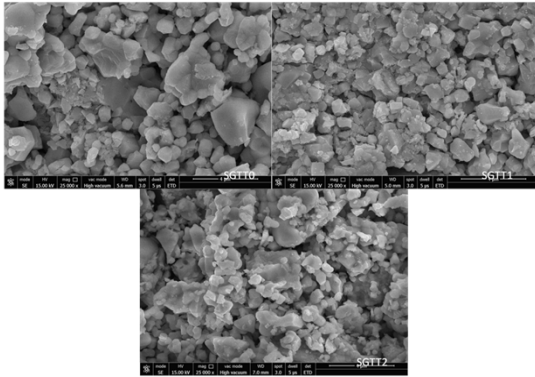


Fig. 2. FESEM Image of  $Sr_{1-a}Gd_aTi_{1-b}Tm_bO_{3-d}$  Samples ( $0 \leq a \leq 0.1, 0 \leq b \leq 0.005$ )

**Electrical/Dielectric Characterization**

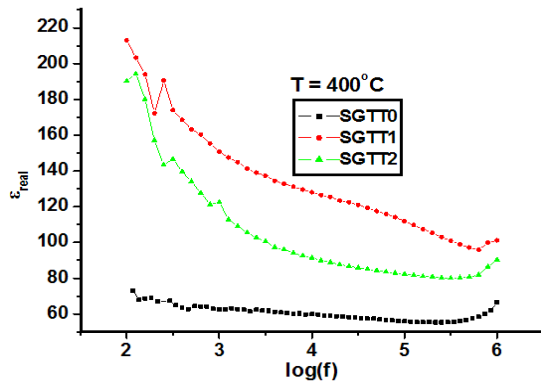


Fig. 3. Variation of Dielectric Constant with Frequency at 400°C for  $Sr_{1-a}Gd_aTi_{1-b}Tm_bO_{3-d}$  Samples ( $0 \leq a \leq 0.1, 0 \leq b \leq 0.005$ )

Dielectric constant measurement done in temperature range 50-400°C and frequency range 1Hz to 1 MHz revealed the decrease in dielectric constant value with frequency and increase in it with temperature. Fig. 3 includes the frequency variation of dielectric constant at temperature 400°C for all the samples; clearly doped samples have higher values than the pure one<sup>14-17</sup>.

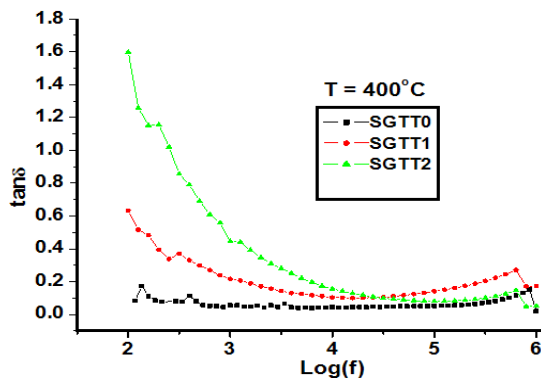


Fig. 4. Variation of Dielectric Loss with Frequency at 400°C for  $Sr_{1-a}Gd_aTi_{1-b}Tm_bO_{3-d}$  Samples ( $0 \leq a \leq 0.1, 0 \leq b \leq 0.005$ )

Figures 4 and 5 include the variation of loss tangent and conductivity, respectively, with frequency at temperature 400°C. Loss tangent factor decreases with frequency whereas conductivity increases. The doped samples showed higher loss factor and conductivity values than the pure one<sup>17-22</sup>.

Cole-Cole plots for all the three samples at temperature 400°C are included in Fig. 6. The grain effects in the prepared samples can be depicted from the presence of semicircle in the plots. The semicircle radius decreases with temperature as well as with doping indicating the decrement in resistance<sup>23</sup>.

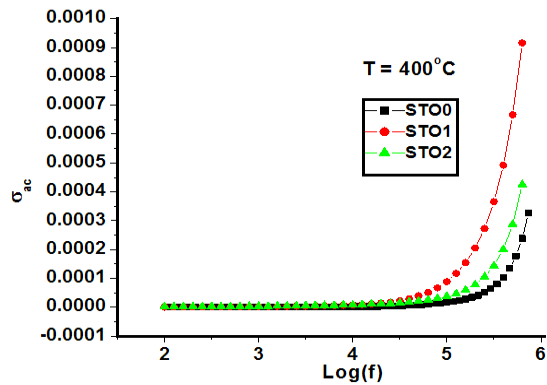


Fig. 5. Variation of ac Conductivity with Frequency at Temperature 400°C for  $Sr_{1-a}Gd_aTi_{1-b}Tm_bO_{3-d}$  Samples ( $0 \leq a \leq 0.1, 0 \leq b \leq 0.005$ )

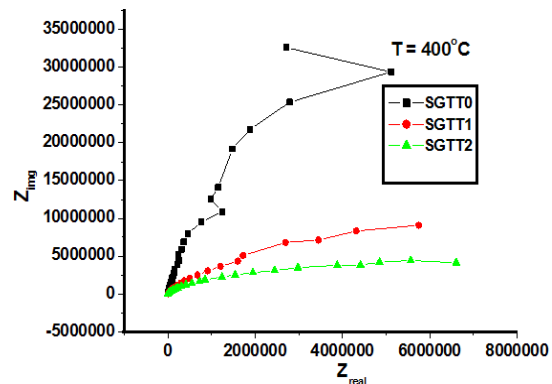


Fig. 6. Cole-Cole Plots between Real Part ( $Z'$ ) and Imaginary Part ( $Z''$ ) of Impedance at 400°C for  $Sr_{1-a}Gd_aTi_{1-b}Tm_bO_{3-d}$  Samples ( $0 \leq a \leq 0.1, 0 \leq b \leq 0.005$ )

**CONCLUSION**

Gadolinium and thulium doped strontium titanates have been synthesized in this work. XRD and SEM/EDX analysis revealed the formation of desired samples with required cubic structure. Doping with 'Gd' led to decrease in lattice parameter

as expected; furthermore the doping led to decrease in grain size revealing the better morphology. Also, the dielectric constant, conductivity etc. showed improvement with 'Gd' and 'Tm' doping.

#### ACKNOWLEDGEMENT

One of the authors Ms. Ramanjeet Kaur highly acknowledges IKGPTU (Inder Kumar Gujral Punjab Technical University), Kapurthala, Punjab,

India for providing facilities in this course. The authors are also very thankful to TEQIP, MHRD/ World Bank Project, IIC, I.I.T. Roorkee, MRC, MNIT Jaipur, Thapar University, Patiala and S B S State Technical Campus, Ferozepur for help and support in this whole work.

#### Conflict of interest

The authors declare that they have no conflict of interest.

#### REFERENCES

1. Minh, N. Q., *Journal of American Ceramic Society.*, **1993**, 76, 563.
2. Singhal, S. C., *MRS Bulletin.*, **2000**, 25, 16.
3. Mukundan, R.; Brosha, E. L.; Garzon, F. H., *Electrochemical and Solid-State Letters.*, **2004**, 7, A5–A7.
4. Cheng, Z.; Zha, S.; Liu, M., *Journal of Electrochemical Society.*, **2006**, 153, A1302–A1309.
5. Zhang, L.; Tosho, T.; Okinaka, N.; Akiyama, T., *Materials Transactions.*, **2007**, 48(8), 2088–2093.
6. Tolczyk, M.; Molin, S.; Gazda, M.; Jasinski, P., *Ceramic Materials.*, **2011**, 63(1), 151–156.
7. Cheng, Z.; Zha, S.; Liu, M., *Journal of Electrochemical Society.*, **2006**, 153, A1302–A1309.
8. Ruiz-Morales, J. C.; Canales-Vázquez, J.; Savaniu, C.; Marrero López, D.; Zhou, W.; Irvine, J. T. S., *Nature.*, **2006**, 439, 568.
9. Hui, S.; Petric, A., *J. Eur. Ceram. Soc.*, **2002**, 22, 1673–1681.
10. Rocca, A.; Licciulli, A.; Politi, M.; Diso, D., International Scholarly Research Network Ceramics., **2012**.
11. Laboratory Module, Indexing X-ray Diffraction Patterns.
12. Shannon, R. D., *Acta Crystallographica*, **1976**, A32, 751–767.
13. Cullity, B. D., Elements of X-ray Diffraction, 2<sup>nd</sup> edition, Addison-Wesley., **1978**.
14. Verma, A.; Thakur, O. P.; Prakash, C.; Goel, T. C.; Mendiratta, R. G., *Material Science and Engineering B.*, **2005**, 116(1).
15. Badapanda, T.; Harichandan, R. K.; Mishra, A.; Anwar, S., *Journal of Advanced Dielectrics.*, **2013**, 3(2), 1350013.
16. Abhijit, P.; Amitabha, B., *Journal of Material Science. Materials in Electronics.*, **2013**, 24, 1855–1862.
17. Li, W.; Ma, Z.; Gao, L.; Wang, F., *Materials.*, **2015**, 8, 1176–1186.
18. Rout, S. K.; Panigrahi, S.; Bera, J., *Indian Journal of Pure & Applied Physics.*, **2004**, 42, 741–744.
19. White, M. A.; Physical Properties of Materials, USA. CRC Press, Boca Raton., **2011**.
20. Naidu, K. C. B.; Sarmash, T. S.; Subbarao, T., *International Journal of Engineering Research & Technology.*, **2014**, 3(1).
21. Badapanda, T.; Harichandan, R. K.; Mishra, A.; Anwar, S., *Processing and Application of Ceramics.*, **2014**, 8(3), 145–153.
22. Karczewski, J.; Riegel, B.; Gazda, M.; Jasinski, P.; Kusz, B., *Journal of Electroceramics.*, **2010**, 24, 326–330.
23. Sahoo, S.; Dash, U.; Parashar, S. K. S.; All, S. M., *Journal of Advanced Ceramics.*, **2013**, 2(3), 291–300.